

ORIGINAL ARTICLE

Revisit of degenerate scales in the BIEM/BEM for 2D elasticity problems

Jeng-Tzong Chen^{a,b}, Wen-Sheng Huang^a, Ying-Te Lee^a, Shyh-Rong Kuo^a, and Shing-Kai Kao^a

^aDepartment of Harbor and River Engineering, National Taiwan Ocean University, Keelung, Taiwan; ^bDepartment of Mechanical and Mechatronic Engineering, National Taiwan Ocean University, Keelung, Taiwan

ABSTRACT

The boundary integral equation method in conjunction with the degenerate kernel, the direct searching technique (singular value decomposition), and the only two-trials technique (2×2 matrix eigenvalue problem) are analytically and numerically used to find the degenerate scales, respectively. In the continuous system of boundary integral equation, the degenerate kernel for the 2D Kelvin solution in the polar coordinates is reviewed and the degenerate kernel in the elliptical coordinates is derived. Using the degenerate kernel, an analytical solution of the degenerate scales for the elasticity problem of circular and elliptical cases is obtained and compared with the numerical result. Further, the triangular case and square case were also numerically demonstrated.

ARTICLE HISTORY

Received 24 February 2015
Accepted 2 July 2015

KEYWORDS

Boundary element method; boundary integral equation method; two-dimensional elasticity; degenerate scale; degenerate kernel; eigenvalue problem

1. Introduction

In mathematical physics, the interior Dirichlet problem exists in a unique solution and the interior Neumann problem for the Laplace equation results in nonunique solutions. Physically speaking, a constrained structure has only one solution. However, rigid body modes can be superimposed in the deformed state of a free-free structure. For the paradox in 2D elasticity problems, not only the wedge problem [1] but also the degenerate scale in the boundary integral equation method (BIEM)/boundary element method (BEM) is due to the incomplete mathematical model [2–8]. It is interesting to find that boundary integral formulation for the 2D constrained structure may result in nonunique solutions for a special size of domain. This outcome cannot be physically realizable because it stems from the range deficiency of an integral operator of the single layer potential. In the BEM after the discretization of the BIEM, rank deficiency in the influence matrix can be found. How to understand the occurring mechanism is an interesting issue.

For scalar and vector fields, the boundary integral equation (BIE) is constructed once the fundamental solution is available. For the 2D Laplace problem, a $\ln r$ term appears in the fundamental solution, since $\ln r$ is not objective once the observer system is changed [9]. This is the original source of the degenerate scale in the BIE for 2D potential and elasticity problems. From another point of view, there are smooth curves on which the trivial boundary Dirichlet data can have nontrivial boundary Neumann data [10].

It is well known that this problem may be encountered in the Laplace [11–14] and plane elasticity problems [13, 15–18]. To avoid the problem, several approaches, namely hypersingular formulation, method of adding a rigid body mode, rank promotion by adding the boundary flux equilibrium, the CHEEF

method, and the Fichera method, were employed to transform an ill-posed model to a well-posed model [19]. Only one degenerate scale for the scalar potential problem was found. However, numerical evidence indicates that two degenerate scales may occur in the 2D elasticity problem. Not only the BEM [14] but also the symmetric Galerkin BEM [17] both result in two degenerate scales. Nevertheless, also in isotropic elasticity, the anti-plane deformation (governed by the Laplace equation) may provide another degenerate scale. Switching to anisotropic materials, the in-plane and anti-plane deformations cannot be generally uncoupled, so that in anisotropic elasticity for 2D geometry we can have up to three degenerate scales [20].

Based on the complex variables, Chen et al. [10] have derived two analytical scales. However, they are different from the one derived by He et al. [6]. It is interesting to find that their kernel functions are different by a constant term of $0.5 \delta_{ij}$ [21]. This reconfirms that degenerate scale depends on the kernel function. Although the method of the complex variable is an elegant and genius approach to find the degenerate scale, a more systematic, logical, and natural way to analytically derive the degenerate scale by using the degenerate kernel is not trivial. Based on the spectral idea, both the kernel and boundary density can be expanded. The fundamental solution has two kinds of expression. One is the closed form and the other is the spectral (separable) form. The latter one can be separated into the source point and field point and it is termed degenerate kernel for the fundamental solution in the mathematical terminology. It is found that degenerate scale results in range deficiency of the single-layer integral operator. Two possibilities can be found. One is the infinite solutions if the forcing vector falls in the range of the operator. The other is no solution once the forcing term is out of the range. The method of complex variables is more simple

and elegant than that of the degenerate kernel. Here, we focus on the defects of the integral equation and provide a new method to link the integral equation and the linear algebra by way of the degenerate kernel. Once the degenerate kernel is available, the BIE is nothing more than a linear algebra [22]. Based on the degenerate kernel, the analytical study for the degenerate scale is possible. This is the main concern of this article. Both the polar coordinates for a circle and the elliptical coordinates for an ellipse are considered.

2. Degenerate kernels for the Kelvin solution

According to the successful experiences of the application in the Laplace problems by using the degenerate kernel, we can clarify why the range of a single-layer integral operator is deficient. In this section, degenerate kernels for the elasticity problem in the polar and elliptical coordinates of a circle and an ellipse are both addressed. The medium is considered to be linearly elastic, isotropic, and homogenous. The governing equation is shown below:

$$(\lambda + G)\nabla(\nabla \cdot \tilde{u}(\mathbf{x})) + G\nabla^2 \tilde{u}(\mathbf{x}) = 0, \mathbf{x} \in D, \quad (1)$$

where $\mathbf{u}(\mathbf{x})$ is the displacement vector, D is the domain of interest, ∇^2 is the Laplace operator, and λ and G are the Lamé constants for the isotropic elasticity.

2.1. Review of the Kelvin solution by using the degenerate kernel in terms of the polar coordinates

In this section, we would like to review the degenerate kernel for the Kelvin solution in terms of the polar coordinates. The closed-form Kelvin solution of the Navier equation is given below:

$$U_{ij}(\mathbf{s}, \mathbf{x}) = -\frac{1}{8\pi G(1-\nu)} \left(\kappa \delta_{ij} \ln r - \frac{y_i y_j}{r^2} \right), \quad (2)$$

where δ_{ij} is the Kronecker delta, ν is the Poisson ratio, $\kappa = (3 - 4\nu)$, $r = |\mathbf{x} - \mathbf{s}|$, and $y_i = x_i - s_i$.

For deriving the degenerate kernel in terms of the polar coordinates, source point \mathbf{s} and collocation point \mathbf{x} are expressed by (R, θ) and (ρ, ϕ) , respectively. It is well known that the position vector of the source point and the collocation point can be represented by $z_s = s_1 + s_2 i = R e^{i\theta}$ and $z_x = x_1 + x_2 i = \rho e^{i\phi}$ in the theory of the complex variables, respectively. The former term ($\ln r$) in the bracket of Eq. (2) is the fundamental solution of the Laplace equation and its degenerate form can be easily found in [12] as follows:

$$\begin{aligned} \ln |\mathbf{x} - \mathbf{s}| &= \ln r \\ &= \begin{cases} \ln R - \sum_{m=1}^{\infty} \frac{1}{m} \left(\frac{\rho}{R}\right)^m \cos(m(\theta - \phi)), & R \geq \rho, \\ \ln \rho - \sum_{m=1}^{\infty} \frac{1}{m} \left(\frac{R}{\rho}\right)^m \cos(m(\theta - \phi)), & R < \rho, \end{cases} \end{aligned} \quad (3)$$

Therefore, the key point of deriving the degenerate kernel for the Kelvin solution is how to expand the term $(y_i y_j / r^2)$ into a separable form. First, we can easily obtain the following

equation:

$$\begin{aligned} \frac{1}{z_x - z_s} &= \frac{1}{(\rho \cos \phi + i\rho \sin \phi) - (R \cos \theta + iR \sin \theta)} \\ &= \frac{y_1 - iy_2}{r^2}. \end{aligned} \quad (4)$$

For the exterior case ($R < \rho$), Eq. (4) can be expanded by using the geometric series as follows:

$$\begin{aligned} \frac{1}{z_x - z_s} &= \frac{1}{z_x} \frac{1}{1 - (z_s/z_x)} \\ &= \frac{1}{z_x} \left[1 + \frac{z_s}{z_x} + \left(\frac{z_s}{z_x}\right)^2 + \left(\frac{z_s}{z_x}\right)^3 + \left(\frac{z_s}{z_x}\right)^4 + \dots \right] \\ &= \frac{1}{\rho} e^{-i\phi} \left[\sum_{m=0}^{\infty} \left(\frac{R}{\rho}\right)^m e^{im(\theta-\phi)} \right]. \end{aligned} \quad (5)$$

After comparing Eq. (4) with Eq. (5), we have:

$$\begin{aligned} \frac{y_1}{r^2} &= \frac{\rho \cos \phi - R \cos \theta}{\rho^2 + R^2 - 2R\rho \cos(\theta - \phi)} \\ &= \frac{1}{\rho} \sum_{m=0}^{\infty} \left(\frac{R}{\rho}\right)^m \cos[m\theta - (m+1)\phi], \end{aligned} \quad (6)$$

$$\begin{aligned} \frac{y_2}{r^2} &= \frac{\rho \sin \phi - R \sin \theta}{\rho^2 + R^2 - 2R\rho \cos(\theta - \phi)} \\ &= \frac{1}{\rho} \sum_{m=0}^{\infty} \left(\frac{R}{\rho}\right)^m \sin[m\theta - (m+1)\phi]. \end{aligned} \quad (7)$$

Then, we can obtain the following equations:

$$\begin{aligned} \frac{y_1^2}{r^2} &= \frac{1}{2} + \sum_{m=0}^{\infty} \frac{1}{2} \left(\frac{R}{\rho}\right)^m \cos[m\theta - (m+2)\phi] \\ &\quad - \sum_{m=0}^{\infty} \frac{1}{2} \left(\frac{R}{\rho}\right)^{m+1} \cos[(m-1)\theta - (m+1)\phi], \end{aligned} \quad (8)$$

$$\begin{aligned} \frac{y_2^2}{r^2} &= \frac{1}{2} - \sum_{m=0}^{\infty} \frac{1}{2} \left(\frac{R}{\rho}\right)^m \cos[m\theta - (m+2)\phi] \\ &\quad + \sum_{m=0}^{\infty} \frac{1}{2} \left(\frac{R}{\rho}\right)^{m+1} \cos[(m-1)\theta - (m+1)\phi], \end{aligned} \quad (9)$$

$$\begin{aligned} \frac{y_1 y_2}{r^2} &= \sum_{m=0}^{\infty} \frac{1}{2} \left(\frac{R}{\rho}\right)^m \sin[m\theta - (m+2)\phi] \\ &\quad + \sum_{m=0}^{\infty} \frac{1}{2} \left(\frac{R}{\rho}\right)^{m+1} \sin[(m-1)\theta - (m+1)\phi]. \end{aligned} \quad (10)$$

For the interior case ($R \geq \rho$), we have:

$$\begin{aligned} \frac{y_1^2}{r^2} &= \frac{1}{2} + \sum_{m=0}^{\infty} \frac{1}{2} \left(\frac{\rho}{R}\right)^m \cos[m\phi - (m+2)\theta] \\ &\quad - \sum_{m=0}^{\infty} \frac{1}{2} \left(\frac{\rho}{R}\right)^{m+1} \cos[(m-1)\phi - (m+1)\theta], \end{aligned} \quad (11)$$

$$\begin{aligned} \frac{y_2^2}{r^2} &= \frac{1}{2} - \sum_{m=0}^{\infty} \frac{1}{2} \left(\frac{\rho}{R}\right)^m \cos [m\phi - (m+2)\theta] \\ &\quad + \sum_{m=0}^{\infty} \frac{1}{2} \left(\frac{\rho}{R}\right)^{m+1} \cos [(m-1)\phi - (m+1)\theta], \end{aligned} \quad (12)$$

$$\begin{aligned} \frac{y_1 y_2}{r^2} &= \sum_{m=0}^{\infty} \frac{1}{2} \left(\frac{\rho}{R}\right)^m \sin [m\phi - (m+2)\theta] \\ &\quad + \sum_{m=0}^{\infty} \frac{1}{2} \left(\frac{\rho}{R}\right)^{m+1} \sin [(m-1)\phi - (m+1)\theta]. \end{aligned} \quad (13)$$

From the above results, the degenerate form of the Kelvin solution $U_{ij}(s, x)$ can be obtained in [23]. The results were also summarized by using the Table of Mathematics [24].

2.2. Derivation of the degenerate kernel for the Kelvin solution in terms of elliptical coordinates

For the elliptical domain, the elliptical coordinates are more suitable to be used for representing the degenerate kernel for the fundamental solution. Therefore, the degenerate kernel for the Kelvin solution in terms of the elliptical coordinates is the main concern in this section. Here, the degenerate kernel of $\ln r$ in the elliptical coordinates can be found [25] as follows:

$$\begin{aligned} &\ln |\mathbf{x} - \mathbf{s}| \\ &= \ln r = \begin{cases} \bar{\xi} + \ln \frac{c}{2} - \sum_{m=1}^{\infty} \frac{2}{m} e^{-m\bar{\xi}} \cosh m\xi \cos m\eta \cos m\bar{\eta} \\ \quad - \sum_{m=1}^{\infty} \frac{2}{m} e^{-m\bar{\xi}} \sinh m\xi \sin m\eta \sin m\bar{\eta}, \quad \bar{\xi} \geq \xi, \\ \xi + \ln \frac{c}{2} - \sum_{m=1}^{\infty} \frac{2}{m} e^{-m\xi} \cosh m\bar{\xi} \cos m\eta \cos m\bar{\eta} \\ \quad - \sum_{m=1}^{\infty} \frac{2}{m} e^{-m\xi} \sinh m\bar{\xi} \sin m\eta \sin m\bar{\eta}, \quad \bar{\xi} < \xi, \end{cases} \end{aligned} \quad (14)$$

where c is the half distance between two foci, and $\mathbf{s} = (\bar{\xi}, \bar{\eta})$ and $\mathbf{x} = (\xi, \eta)$ are positions of the source point \mathbf{s} and collocation point \mathbf{x} in the elliptical coordinates, respectively. The relationship between the Cartesian and elliptical coordinates is given below:

$$x_1 = c \cosh \xi \cos \eta, \quad x_2 = c \sinh \xi \sin \eta. \quad (15)$$

Based on the chain rule, we have:

$$\begin{aligned} \frac{\partial}{\partial x_1} &= \frac{c \sinh \xi \cos \eta}{J^2} \frac{\partial}{\partial \xi} - \frac{c \cosh \xi \sin \eta}{J^2} \frac{\partial}{\partial \eta}, \\ \frac{\partial}{\partial x_2} &= \frac{c \cosh \xi \sin \eta}{J^2} \frac{\partial}{\partial \xi} + \frac{c \sinh \xi \cos \eta}{J^2} \frac{\partial}{\partial \eta}, \end{aligned} \quad (16)$$

where J is a Jacobian term and

$$J = c\sqrt{\sinh^2 \xi + \sin^2 \eta}. \quad (17)$$

From Eq. (14), we can easily determine the following equations:

$$\frac{\partial(\ln r)}{\partial \xi} = \begin{cases} -2 \sum_{m=1}^{\infty} e^{-m\bar{\xi}} \sinh m\xi \cos m\eta \cos m\bar{\eta} \\ \quad -2 \sum_{m=1}^{\infty} e^{-m\bar{\xi}} \cosh m\xi \sin m\eta \sin m\bar{\eta}, \quad \bar{\xi} \geq \xi, \\ 1 + 2 \sum_{m=1}^{\infty} e^{-m\xi} \cosh m\bar{\xi} \cos m\eta \cos m\bar{\eta} \\ \quad + 2 \sum_{m=1}^{\infty} e^{-m\xi} \sinh m\bar{\xi} \sin m\eta \sin m\bar{\eta}, \quad \bar{\xi} < \xi, \end{cases} \quad (18)$$

$$\frac{\partial(\ln r)}{\partial \eta} = \begin{cases} 2 \sum_{m=1}^{\infty} e^{-m\bar{\xi}} \cosh m\xi \sin m\eta \cos m\bar{\eta} \\ \quad -2 \sum_{m=1}^{\infty} e^{-m\bar{\xi}} \sinh m\xi \cos m\eta \sin m\bar{\eta}, \quad \bar{\xi} \geq \xi, \\ 2 \sum_{m=1}^{\infty} e^{-m\xi} \cosh m\bar{\xi} \sin m\eta \cos m\bar{\eta} \\ \quad -2 \sum_{m=1}^{\infty} e^{-m\xi} \sinh m\bar{\xi} \cos m\eta \sin m\bar{\eta}, \quad \bar{\xi} < \xi. \end{cases} \quad (19)$$

For the gradient, we have:

$$\frac{\partial \ln r}{\partial x_1} = \frac{y_1}{r^2}, \quad \frac{\partial \ln r}{\partial x_2} = \frac{y_2}{r^2}. \quad (20)$$

After combining Eqs. (15)–(20), the separable form of the term $(y_i y_j / r^2)$ is derived as follows:

$$\begin{aligned} \frac{y_1^2}{r^2} &= (c \cosh \xi \cos \eta - c \cosh \bar{\xi} \cos \bar{\eta}) \\ &\quad \left[-\frac{c}{J^2} \sum_{m=1}^{\infty} e^{-m\bar{\xi}} \cosh(m+1)\xi \cos(m-1)\eta \cos m\bar{\eta} \right. \\ &\quad + \frac{c}{J^2} \sum_{m=1}^{\infty} e^{-m\bar{\xi}} \cosh(m-1)\xi \cos(m+1)\eta \cos m\bar{\eta} \\ &\quad - \frac{c}{J^2} \sum_{m=1}^{\infty} e^{-m\bar{\xi}} \sinh(m+1)\xi \sin(m-1)\eta \sin m\bar{\eta} \\ &\quad \left. + \frac{c}{J^2} \sum_{m=1}^{\infty} e^{-m\bar{\xi}} \sinh(m-1)\xi \sin(m+1)\eta \sin m\bar{\eta} \right], \end{aligned} \quad (21)$$

$$\begin{aligned} \frac{y_2^2}{r^2} &= (c \sinh \xi \sin \eta - c \sinh \bar{\xi} \sin \bar{\eta}) \\ &\quad \left[\frac{c}{J^2} \sum_{m=1}^{\infty} e^{-m\bar{\xi}} \sinh(m+1)\xi \cdot \sin(m-1)\eta \cos m\bar{\eta} \right. \\ &\quad \left. - \frac{c}{J^2} \sum_{m=1}^{\infty} e^{-m\bar{\xi}} \sinh(m-1)\xi \cdot \sin(m+1)\eta \cos m\bar{\eta} \right] \end{aligned}$$

$$\begin{aligned} & -\frac{c}{j^2} \sum_{m=1}^{\infty} e^{-m\bar{\xi}} \cosh(m+1)\xi \cdot \cos(m-1)\eta \sin m\bar{\eta} \\ & + \frac{c}{j^2} \sum_{m=1}^{\infty} e^{-m\bar{\xi}} \cosh(m-1)\xi \cdot \cos(m+1)\eta \sin m\bar{\eta} \end{aligned} \quad (22)$$

$$\begin{aligned} \frac{y_1 y_2}{r^2} &= (c \sinh \xi \sin \eta - c \sinh \bar{\xi} \sin \bar{\eta}) \\ & \left[-\frac{c}{j^2} \sum_{m=1}^{\infty} e^{-m\bar{\xi}} \cosh(m+1)\xi \cos(m-1)\eta \cos m\bar{\eta} \right. \\ & + \frac{c}{j^2} \sum_{m=1}^{\infty} e^{-m\bar{\xi}} \cosh(m-1)\xi \cos(m+1)\eta \cos m\bar{\eta} \\ & - \frac{c}{j^2} \sum_{m=1}^{\infty} e^{-m\bar{\xi}} \sinh(m+1)\xi \sin(m-1)\eta \sin m\bar{\eta} \\ & \left. + \frac{c}{j^2} \sum_{m=1}^{\infty} e^{-m\bar{\xi}} \sinh(m-1)\xi \sin(m+1)\eta \sin m\bar{\eta} \right], \end{aligned} \quad (23)$$

for the interior case ($\bar{\xi} \geq \xi$), and

$$\begin{aligned} \frac{y_1^2}{r^2} &= (c \cosh \xi \cos \eta - c \cosh \bar{\xi} \cos \bar{\eta}) \left[\frac{c \sinh \xi \cos \eta}{j^2} \right. \\ & + \frac{c}{j^2} \sum_{m=1}^{\infty} e^{-(m-1)\xi} \cosh m\bar{\xi} \cos(m+1)\eta \cos m\bar{\eta} \\ & - \frac{c}{j^2} \sum_{m=1}^{\infty} e^{-(m+1)\xi} \cosh m\bar{\xi} \cos(m-1)\eta \cos m\bar{\eta} \\ & + \frac{c}{j^2} \sum_{m=1}^{\infty} e^{-(m-1)\xi} \sinh m\bar{\xi} \sin(m+1)\eta \sin m\bar{\eta} \\ & \left. - \frac{c}{j^2} \sum_{m=1}^{\infty} e^{-(m+1)\xi} \sinh m\bar{\xi} \sin(m-1)\eta \sin m\bar{\eta} \right], \end{aligned} \quad (24)$$

$$\begin{aligned} \frac{y_2^2}{r^2} &= (c \sinh \xi \sin \eta - c \sinh \bar{\xi} \sin \bar{\eta}) \left[\frac{c \cosh \xi \sin \eta}{j^2} \right. \\ & + \frac{c}{j^2} \sum_{m=1}^{\infty} e^{-(m-1)\xi} \cosh m\bar{\xi} \sin(m+1)\eta \cos m\bar{\eta} \\ & - \frac{c}{j^2} \sum_{m=1}^{\infty} e^{-(m+1)\xi} \cosh m\bar{\xi} \sin(m-1)\eta \cos m\bar{\eta} \\ & - \frac{c}{j^2} \sum_{m=1}^{\infty} e^{-(m-1)\xi} \sinh m\bar{\xi} \cos(m+1)\eta \sin m\bar{\eta} \\ & \left. + \frac{c}{j^2} \sum_{m=1}^{\infty} e^{-(m+1)\xi} \sinh m\bar{\xi} \cos(m-1)\eta \sin m\bar{\eta} \right], \end{aligned} \quad (25)$$

$$\begin{aligned} \frac{y_1 y_2}{r^2} &= (c \sinh \xi \sin \eta - c \sinh \bar{\xi} \sin \bar{\eta}) \left[\frac{c \sinh \xi \cos \eta}{j^2} \right. \\ & + \frac{c}{j^2} \sum_{m=1}^{\infty} e^{-(m-1)\xi} \cosh m\bar{\xi} \cos(m+1)\eta \cos m\bar{\eta} \\ & - \frac{c}{j^2} \sum_{m=1}^{\infty} e^{-(m+1)\xi} \cosh m\bar{\xi} \cos(m-1)\eta \cos m\bar{\eta} \\ & + \frac{c}{j^2} \sum_{m=1}^{\infty} e^{-(m-1)\xi} \sinh m\bar{\xi} \sin(m+1)\eta \sin m\bar{\eta} \\ & \left. - \frac{c}{j^2} \sum_{m=1}^{\infty} e^{-(m+1)\xi} \sinh m\bar{\xi} \sin(m-1)\eta \sin m\bar{\eta} \right], \end{aligned} \quad (26)$$

for the exterior case ($\bar{\xi} < \xi$). Therefore, the degenerate form of kernels $U_{ij}(\mathbf{s}, \mathbf{x})$ for the elliptical case can be obtained by using the above formulae and is included in the Appendix. Besides, the other kernels can be straightforwardly derived according to the traction operator to $U_{ij}(\mathbf{s}, \mathbf{x})$ [26]. In the literature, the degenerate kernel for the Kelvin solution in terms of the elliptical coordinates was not found to the authors' best knowledge. It may be the first time that the degenerate kernel is derived in terms of the elliptical coordinates. Although the form seems more lengthy and complicated than that of the circular case, it is useful for the analytical study for the degenerate scale of an ellipse in the BIEM/BEM.

3. Derivation of analytical degenerate scales of a circle and an ellipse

In a 2D Laplace problem with special boundary subjected to the Dirichlet boundary condition, the BIEM/BEM may lead to the nonunique solutions. Nonunique solutions are not physically realizable. Owing to the fundamental solution $\ln r$, the range of the single-layer integral operator in the BIE may lose the constant term on the specific size [19]. Range deficiency occurs on the specific size, which is called the degenerate scale. It can be analytically examined by using the degenerate kernel. Based on this experience, we extend the 2D elasticity problem and examine the occurring mechanism of the degenerate scale.

3.1. Degenerate scales on the circular domain for a 2D elasticity problem

In this article, we focus on the interior problem of the specified boundary displacement only since it results in a degenerate scale. Single-layer integral representation for the solution yields the Fredholm integral equations of the first kind as given below:

$$\int_B U_{ij}(\mathbf{s}, \mathbf{x}) \alpha_j(s) dB(\mathbf{s}) = u_i(\mathbf{x}), \quad \mathbf{x} \in D, \quad (27)$$

where $i = 1, 2$, $j = 1, 2$, and $U_{ij}(\mathbf{s}, \mathbf{x})$ is the Kelvin solution. According to the above section of the Kelvin solution by using the degenerate kernel in terms of the polar coordinates, a closed-form kernel can be represented to a degenerate form. The

unknown boundary densities $\alpha_j(\mathbf{s})$ and the given boundary conditions $f_i(\mathbf{x})$ along the boundary can be expressed by using the Fourier expansion as shown below:

$$\alpha_j(\mathbf{s}) = a_0^{(j)} + \sum_{n=1}^{\infty} a_n^{(j)} \cos(n\theta) + b_n^{(j)} \sin(n\theta), \quad 0 \leq \theta \leq 2\pi, \quad (28)$$

$$f_i(\mathbf{x}) = p_0^{(i)} + \sum_{n=1}^{\infty} p_n^{(i)} \cos(n\phi) + q_n^{(i)} \sin(n\phi), \quad 0 \leq \phi \leq 2\pi, \quad (29)$$

where $a_0^{(j)}$, $a_n^{(j)}$, and $b_n^{(j)}$ are unknown coefficients; $p_0^{(i)}$, $p_n^{(i)}$, and $q_n^{(i)}$ are known coefficients from the specified boundary displacement. After substituting the degenerate kernel for the Kelvin solution and the Fourier series expansions for the boundary densities and matching the boundary conditions, we can determine the unknown coefficients as:

$$a_0^{(1)} = \frac{8G(1-\nu)}{(1-2\kappa \ln R_c)R_c} p_0^{(1)}, \quad (30)$$

$$a_1^{(1)} = \frac{2G(1-\nu)}{(1-2\nu)\kappa R_c} \left((5-8\nu) p_1^{(1)} + q_1^{(2)} \right), \quad (31)$$

$$a_n^{(1)} = \frac{8nG(1-\nu)}{\kappa R_c} p_n^{(1)}, \quad n \geq 2, \quad (32)$$

$$b_1^{(1)} = \frac{G}{\kappa R_c} \left((7-8\nu) q_1^{(1)} + p_1^{(2)} \right), \quad (33)$$

$$b_n^{(1)} = \frac{8nG(1-\nu)}{\kappa R_c} q_n^{(1)}, \quad n \geq 2, \quad (34)$$

$$a_0^{(2)} = \frac{8\pi G(1-\nu)}{(1-2\kappa \ln R_c)R_c} p_0^{(2)}, \quad (35)$$

$$a_1^{(2)} = \frac{G}{\kappa R_c} \left((7-8\nu) p_1^{(2)} + q_1^{(1)} \right), \quad (36)$$

$$a_n^{(2)} = \frac{8nG(1-\nu)}{\kappa R_c} p_n^{(2)}, \quad n \geq 2, \quad (37)$$

$$b_1^{(2)} = \frac{2G(1-\nu)}{(1-2\nu)\kappa R_c} \left((5-8\nu) q_1^{(2)} + p_1^{(1)} \right), \quad (38)$$

$$b_n^{(2)} = \frac{8nG(1-\nu)}{\kappa R_c} q_n^{(2)}, \quad n \geq 2. \quad (39)$$

Here, R_c is the radius of circular domain. When the denominator $(1-2\kappa \ln R_c)$ in Eqs. (30) and (35) are equal to zero, both coefficients $a_0^{(1)}$ and $a_0^{(2)}$ cannot be determined. It means that the BIE has nonunique solutions when a degenerate scale is considered. Therefore, two analytical values for degenerate scales of a circular domain for the 2D elasticity problem are the same and reduce to one by:

$$R_d = e^{\frac{1}{2\kappa}}, \quad (40)$$

where R_d is the degenerate scale for the radius of a circle.

3.2. Degenerate scales of the elliptical domain for a 2D elasticity problem

Following the successful experience by using the single-layer formulation to deal with Laplace problems and the circular case in the Navier equation, we could find that the degenerate scale is due to the logarithmic term in the closed-form fundamental solution since it is not objective. Similarly, for analytically deriving the degenerate scale of an elliptical domain, the unknown boundary densities $\alpha_j(\mathbf{s})$ and the given boundary conditions $f_i(\mathbf{x})$ can be expanded by using the eigenfunction representation as shown below:

$$\alpha_j(\mathbf{s}) = \frac{1}{J_s} (a_0^{(j)} + \sum_{n=1}^{\infty} a_n^{(j)} \cos(n\bar{\eta}) + b_n^{(j)} \sin(n\bar{\eta})), \quad 0 \leq \bar{\eta} \leq 2\pi, \quad (41)$$

$$f_i(\mathbf{x}) = p_0^{(i)} + \sum_{n=1}^{\infty} p_n^{(i)} \cos(n\eta) + q_n^{(i)} \sin(n\eta), \quad 0 \leq \eta \leq 2\pi, \quad (42)$$

where $a_0^{(j)}$, $a_n^{(j)}$, and $b_n^{(j)}$ are unknown coefficients, the coefficients $p_0^{(i)}$, $p_n^{(i)}$, and $q_n^{(i)}$ are given from the boundary condition, and the Jacobian term for the source point is given by:

$$J_s = c\sqrt{\sinh^2 \bar{\xi} + \sin^2 \bar{\eta}}. \quad (43)$$

Although the degenerate kernel looks tedious, we only need to care about the logarithmic term to derive the analytic degenerate scale for the elliptical domain. The cause of the degenerate scale in the BIEM/BEM is that the representation of solution may lose the constant term in the range of the single-layer integral operator. For simplification, we design a boundary condition of a rigid body displacement as follows:

$$u_1(\mathbf{x}) = f_1(\mathbf{x}) = p_0^{(1)}, \quad \mathbf{x} \in B \quad (44)$$

and

$$u_2(\mathbf{x}) = f_2(\mathbf{x}) = p_0^{(2)}, \quad \mathbf{x} \in B, \quad (45)$$

where $p_0^{(1)}$ and $p_0^{(2)}$ are two constants.

By substituting the degenerate kernel into the fundamental solution and matching B.C. in Eq. (44) in companion with the following identities:

$$\cosh 3\bar{\xi} = 4\cosh^3 \bar{\xi} - 3\cosh \bar{\xi}, \quad (46)$$

$$\cos 2\eta = 2\cos^2 \eta - 1, \quad (47)$$

the unknown constant term $a_0^{(1)}$ can be determined by:

$$\frac{1}{8G(1-\nu)} \left[-2\kappa \left(\bar{\xi} + \ln \frac{c}{2} \right) + 2e^{-\bar{\xi}} \cosh \bar{\xi} \right] a_0^{(1)} = p_0^{(1)}. \quad (48)$$

According to some relationships between the geometry parameters and elliptical coordinates:

$$\bar{\xi} = \tanh^{-1} \left(\frac{b}{a} \right) = \ln \left(\frac{a+b}{c} \right), \quad (49)$$

$$\cosh \bar{\xi} = \frac{a}{c}, \quad (50)$$

$$\sinh \bar{\xi} = \frac{b}{c}, \quad (51)$$

$$e^{-\bar{\xi}} = \cosh \bar{\xi} - \sinh \bar{\xi} = \frac{a-b}{c}. \quad (52)$$

We can obtain the coefficient $a_0^{(1)}$:

$$a_0^{(1)} = \frac{8G(1-\nu)}{-2\kappa \left(\ln \frac{a+b}{2} \right) + \frac{2a}{a+b}} p_0^{(1)}, \quad (53)$$

where a and b are the length of semi-major axis and semi-minor axis in the elliptical domain, respectively.

Similarly, we obtain:

$$a_0^{(2)} = \frac{8G(1-\nu)}{-2\kappa \left(\ln \frac{a+b}{2} \right) + \frac{2b}{a+b}} p_0^{(2)}, \quad (54)$$

for the vertical direction of rigid body displacement.

When the size of the domain is a degenerate scale, Eqs. (53) and (54) yield nonunique solutions of $a_0^{(1)}$ and $a_0^{(2)}$ due to:

$$-2(3-4\nu) \left(\ln \frac{a+b}{2} \right) + \frac{2a}{a+b} = 0 \quad (55)$$

and

$$-2(3-4\nu) \left(\ln \frac{a+b}{2} \right) + \frac{2b}{a+b} = 0. \quad (56)$$

According to Eqs. (55) and (56), it is found that a and b can be interchanged.

4. Numerical examination of degenerate scales by using the direct searching technique of only two ordinary trials

4.1. Direct searching technique to find the degenerate scale

In the discrete BEM system, Eq. (27) is rewritten as follows:

$$\mathbf{U} \underline{\alpha} = \underline{u} \quad (57)$$

where the influence matrix \mathbf{U} is obtained after the discretization of Eq. (27), $\underline{\alpha}$ is the vector of unknown boundary density, and \underline{u} is the vector of boundary displacement. The influence matrix \mathbf{U} in the BEM can be expressed as:

$$\mathbf{U} = \begin{bmatrix} \mathbf{U}_{11} & \mathbf{U}_{12} \\ \mathbf{U}_{21} & \mathbf{U}_{22} \end{bmatrix}, \quad (58)$$

where the dimension of \mathbf{U} is $2n \times 2n$ and submatrices \mathbf{U}_{ij} is $n \times n$. When the ordinary scale case is considered, the boundary densities could be uniquely obtained. When a degenerate scale happens, the influence matrix \mathbf{U} is singular (the minimum singular value is zero) and the boundary densities could not be determined. Although the direct searching scheme can straightforward find the degenerate scale, it is not efficient due to many trials.

4.2. Only two-trials to find degenerate scales

If the degenerate scales are found by using the direct searching technique, it is time consuming. According to the only one-trial technique [12] in the 2D Laplace problems, we extended this

idea to the 2D elasticity problems. Although the only one-trial technique is deduced in the continuous and the discrete system for Laplace problems, we extend to only two-trials for the elasticity problem.

For any 2D elasticity problem with a simply connected domain subjected to the specified displacement, there exists a unique solution. In the implementation of the BEM, the boundary of Eq. (57) is divided into n elements. The vector \underline{l} is shown as:

$$\underline{l} = \langle l_1 \ l_2 \ l_3 \ \cdots \ l_n \rangle^T, \quad (59)$$

where the component l_i means the length of the i th boundary element.

By specifying the two cases of the different rigid body displacement,

$$\underline{u}_1 = \begin{Bmatrix} \underline{\xi} \\ \underline{0} \end{Bmatrix}, \quad (60)$$

for case 1 of the rigid body mode in the x_1 direction, and

$$\underline{u}_2 = \begin{Bmatrix} \underline{0} \\ \underline{\xi} \end{Bmatrix}, \quad (61)$$

for case 2 of the rigid body mode in the x_2 direction, where we assume the rigid body displacement $\underline{\xi} = \langle 1 \ 1 \ 1 \ \cdots \ 1 \rangle^T$.

According to Eqs. (57), (60), and (61) for an ordinary scale, we obtain the unique solution in the following equations:

$$\mathbf{U} \begin{Bmatrix} \underline{\alpha}_{11} \\ \underline{\alpha}_{21} \end{Bmatrix} = \mathbf{U} \underline{\alpha}^{(1)} = \begin{Bmatrix} \underline{\xi} \\ \underline{0} \end{Bmatrix}, \quad (62)$$

$$\mathbf{U} \begin{Bmatrix} \underline{\alpha}_{12} \\ \underline{\alpha}_{22} \end{Bmatrix} = \mathbf{U} \underline{\alpha}^{(2)} = \begin{Bmatrix} \underline{0} \\ \underline{\xi} \end{Bmatrix}. \quad (63)$$

In Eqs. (62) and (63), $\underline{\alpha}_{ij}$ is the boundary density corresponding to the j th case ($j = 1, 2$) and i denotes the direction of x_i ($i = 1, 2$). According to Eqs. (62) and (63), any boundary density vector $\underline{\varphi}_i$ could be expressed as follows:

$$\begin{Bmatrix} \underline{\varphi}_1 \\ \underline{\varphi}_2 \end{Bmatrix} = \begin{bmatrix} \underline{\alpha}_{11} & \underline{\alpha}_{12} \\ \underline{\alpha}_{21} & \underline{\alpha}_{22} \end{bmatrix} \begin{Bmatrix} \beta_1 \\ \beta_2 \end{Bmatrix} = \beta_1 \underline{\alpha}^{(1)} + \beta_2 \underline{\alpha}^{(2)} \quad (64)$$

By scaling the ordinary boundary B to a new boundary B^* and expressing the original boundary in terms of $f(x_1, x_2) = 0$, $(x_1, x_2) \in B$, we have a new closed boundary curve boundary by:

$$f(d^*x_1, d^*x_2) = 0, \quad (d^*x_1, d^*x_2) \in B^*, \quad (65)$$

where d^* is the expansion ratio. In the expanded boundary, the kernel function for the boundary point can be expressed by:

$$U_{ij}(d^*\mathbf{s}, d^*\mathbf{x}) = U_{ij}(\mathbf{s}, \mathbf{x}) - g_0 \ln d^* \delta_{ij}, \quad \mathbf{x} \in B, \mathbf{s} \in B. \quad (66)$$

This modified equation is the same as that shown in [8].

Equation (58) can be rewritten as shown below:

$$\mathbf{U}^* = \begin{bmatrix} \mathbf{U}_{11} & \mathbf{U}_{12} \\ \mathbf{U}_{21} & \mathbf{U}_{22} \end{bmatrix} - g_0 \ln d^* \begin{bmatrix} \mathbf{E} & \mathbf{0} \\ \mathbf{0} & \mathbf{E} \end{bmatrix}, \quad (67)$$

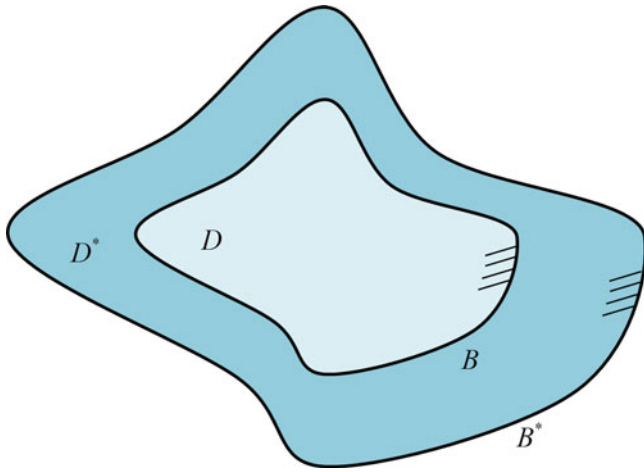


Figure 1. An ordinary scale (D, B) and the degenerate scale (D^*, B^*).

where $g_0 = \frac{(3-4\nu)}{8\pi G(1-\nu)}$ and $\mathbf{E} = \underline{\underline{e}} \underline{\underline{l}}^T$.

Two boundary curves, B and B^* , are shown in **Figure 1**. By mapping the boundary with the nondegenerate (ordinary) scale to the boundary with the degenerate scale, we have the trivial solution of the following system:

$$\begin{bmatrix} \mathbf{U}_{11}^* & \mathbf{U}_{12}^* \\ \mathbf{U}_{21}^* & \mathbf{U}_{22}^* \end{bmatrix} \begin{Bmatrix} \underline{\underline{\varphi}}_1 \\ \underline{\underline{\varphi}}_2 \end{Bmatrix} = \begin{Bmatrix} \underline{\underline{0}} \\ \underline{\underline{0}} \end{Bmatrix}. \quad (68)$$

Substituting **Eqs. (64) and (67)** into **Eq. (68)**, we have:

$$\mathbf{U} \begin{bmatrix} \underline{\underline{\alpha}}_{11} & \underline{\underline{\alpha}}_{12} \\ \underline{\underline{\alpha}}_{21} & \underline{\underline{\alpha}}_{22} \end{bmatrix} \begin{Bmatrix} \beta_1 \\ \beta_2 \end{Bmatrix} - g_0 \ln d^* \begin{bmatrix} \mathbf{E} & \mathbf{0} \\ \mathbf{0} & \mathbf{E} \end{bmatrix} \begin{Bmatrix} \beta_1 \\ \beta_2 \end{Bmatrix} = \begin{Bmatrix} \underline{\underline{0}} \\ \underline{\underline{0}} \end{Bmatrix}. \quad (69)$$

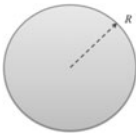
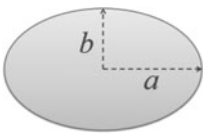
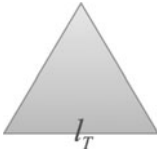
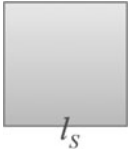
We set a cofactor matrix \mathbf{P} as follows:

$$\mathbf{U} \begin{bmatrix} \underline{\underline{\alpha}}_{11} & \underline{\underline{\alpha}}_{12} \\ \underline{\underline{\alpha}}_{21} & \underline{\underline{\alpha}}_{22} \end{bmatrix} = \begin{bmatrix} \underline{\underline{e}} & \underline{\underline{0}} \\ \underline{\underline{0}} & \underline{\underline{e}} \end{bmatrix} = \mathbf{P}, \quad (70)$$

and

$$\begin{bmatrix} \mathbf{E} & \mathbf{0} \\ \mathbf{0} & \mathbf{E} \end{bmatrix} = \begin{bmatrix} \underline{\underline{e}} & \underline{\underline{0}} \\ \underline{\underline{0}} & \underline{\underline{e}} \end{bmatrix} \begin{bmatrix} \underline{\underline{l}}^T & \underline{\underline{0}} \\ \underline{\underline{0}} & \underline{\underline{l}}^T \end{bmatrix} = \mathbf{P} \begin{bmatrix} \underline{\underline{l}}^T & \underline{\underline{0}} \\ \underline{\underline{0}} & \underline{\underline{l}}^T \end{bmatrix}. \quad (71)$$

Table 1. Degenerate scales for four domains by using three approaches.

				
	Circle	Ellipse ($b = 0.5a$)	Triangle	Square
Analytical degenerate scale (degenerate kernel)	$R_d = 1.28403$	$b_1^* = 0.78757$ $b_2^* = 0.93041$	N.A.	N.A.
Numerical degenerate scale (two-trials technique) (2×2 eigensystem)	$R_d = 1.28415$	$b_1^* = 0.78765$ $b_2^* = 0.93050$	$l_T^* = 3.00004$	$l_S^* = 2.15823$
Numerical degenerate scale (direct searching technique)	$R_d = 1.28400$	$b_1^* = 0.78760$ $b_2^* = 0.93040$	$l_T^* = 3.00030$	$l_S^* = 2.16000$

Therefore, **Eq. (69)** yields:

$$\mathbf{P} \left(\begin{Bmatrix} \beta_1 \\ \beta_2 \end{Bmatrix} - g_0 \ln d^* \begin{bmatrix} k_{11} & k_{12} \\ k_{21} & k_{22} \end{bmatrix} \begin{Bmatrix} \beta_1 \\ \beta_2 \end{Bmatrix} \right) = \begin{Bmatrix} \underline{\underline{0}} \\ \underline{\underline{0}} \end{Bmatrix}, \quad (72)$$

where $k_{ij} = \underline{\underline{l}}^T \underline{\underline{\alpha}}_{ij}$ and k_{ij} is a real-valued coefficient and $i = 1, 2$, $j = 1, 2$. The matrix \mathbf{K} is composed of element k_{ij} as shown below:

$$\mathbf{K} = \begin{bmatrix} k_{11} & k_{12} \\ k_{21} & k_{22} \end{bmatrix}. \quad (73)$$

It is interesting to find that the matrix \mathbf{K} is the second-order tensor. The numerical proof is included in the numerical examples.

According to **Eq. (72)**, we can reduce the degenerate-scale problem in 2D plane elasticity to a 2×2 eigenproblem as shown below:

$$\mathbf{K} \begin{Bmatrix} \beta_1 \\ \beta_2 \end{Bmatrix} = \begin{bmatrix} k_{11} & k_{12} \\ k_{21} & k_{22} \end{bmatrix} \begin{Bmatrix} \beta_1 \\ \beta_2 \end{Bmatrix} = \frac{1}{g_0 \ln d^*} \begin{Bmatrix} \beta_1 \\ \beta_2 \end{Bmatrix}. \quad (74)$$

The degenerate scale is d^*B once eigenvalue is obtained.

5. Numerical examples

In this section, we would like to apply three approaches to detect the degenerate scale in four simple cases: a circle, an ellipse, a triangle, and a square. For the numerical implementation, we set the Lamé constants G, ν and the constant g_0 as 1, 0.25, and 0.1061, respectively. The number of boundary elements is 120. All of the results are included in **Table 1**.

5.1. Degenerate scales of a circle

First, we consider the problem of a circle as shown in **Figure 2**, and the radius R_c of the circle is given to be 1.

According to **Section 3**, we analytically obtain analytical degenerate scales by using the degenerate kernel. Then, two trials of the indirect BEM yield:

$$\mathbf{K} = \begin{bmatrix} 37.68376 & 0.0000 \\ 0.0000 & 37.68376 \end{bmatrix}, \quad (75)$$

and the expansion ratio is found to be $d_1^* = 1.28415$. Therefore, the degenerate scale of a circular domain is 1.28415, which

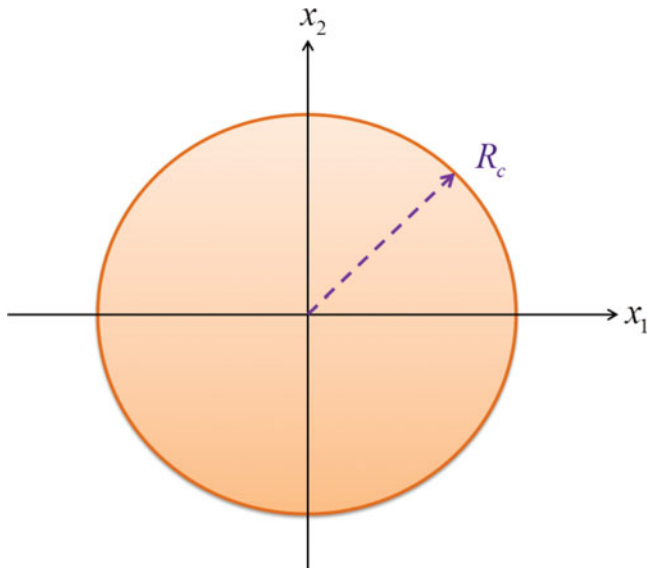


Figure 2. A plane elasticity problem of a circular domain.

matches well with the analytical degenerate scale of 1.28403. According to the direct searching technique, we find that the degenerate scale of radices is 1.28400. The result is shown in Figure 3.

5.2. Degenerate scales of an ellipse

In the elliptical case, we consider the three observer systems (0° , -30° , -60°) to check the second-order tensor property of \mathbf{K} matrix as shown in Figure 4. The ratio of the semi-minor axis b to the semi-major axis a is 0.5 and b is equal to 1.

According to Section 3, we obtain analytical degenerate scales by using the degenerate kernel. We find that the degenerate scales in the three situations of different angles are all the same. By using the two-trials of the indirect BEM with respect to three

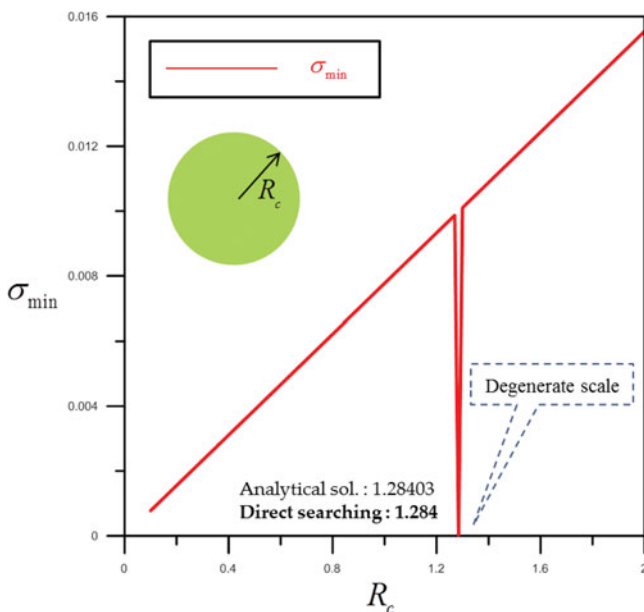


Figure 3. The minimum singular value vs. the length of radius by using the direct searching technique.

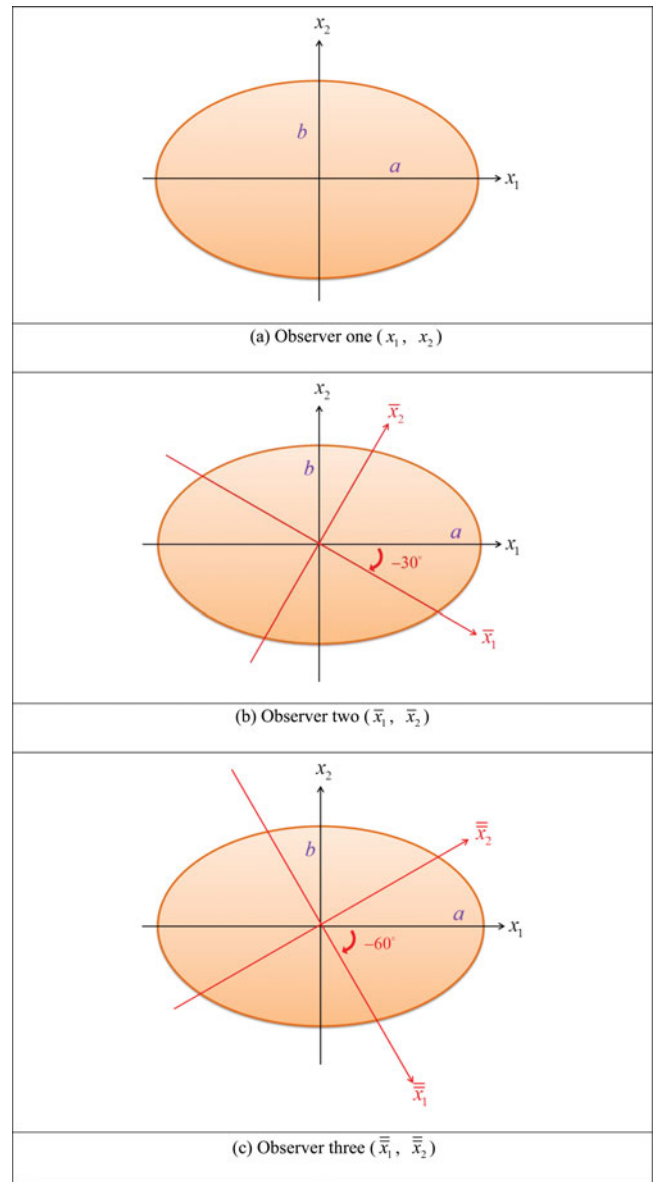


Figure 4. A plane elasticity problem using three observer systems.

observer systems, we have:

$$\mathbf{K}_{0^\circ} = \begin{bmatrix} -130.84343 & 0.0000 \\ 0.00000 & -39.48407 \end{bmatrix}, 0^\circ \text{ observer}, \quad (76)$$

$$\mathbf{K}_{30^\circ} = \begin{bmatrix} -107.99906 & -39.55736 \\ -39.55736 & -62.32206 \end{bmatrix}, -30^\circ \text{ observer}, \quad (77)$$

$$\mathbf{K}_{60^\circ} = \begin{bmatrix} -62.32206 & -39.55736 \\ -39.55736 & -107.99906 \end{bmatrix}, -60^\circ \text{ observer}. \quad (78)$$

We can obtain the same eigenvalues of expansion ratios, $d_1^* = 0.93050$ and $d_2^* = 0.78765$. Therefore, the degenerate scales of an elliptical domain are 0.93050 and 0.78765, which match well with the analytical degenerate scales of 0.93041 and 0.78757.

According to the direct searching technique, we find the degenerate scales of 0.93040 and 0.78760. The result of this technique is shown in Figure 5. It is interesting to find that three \mathbf{K} matrices obey the second-order tensor transformation as shown

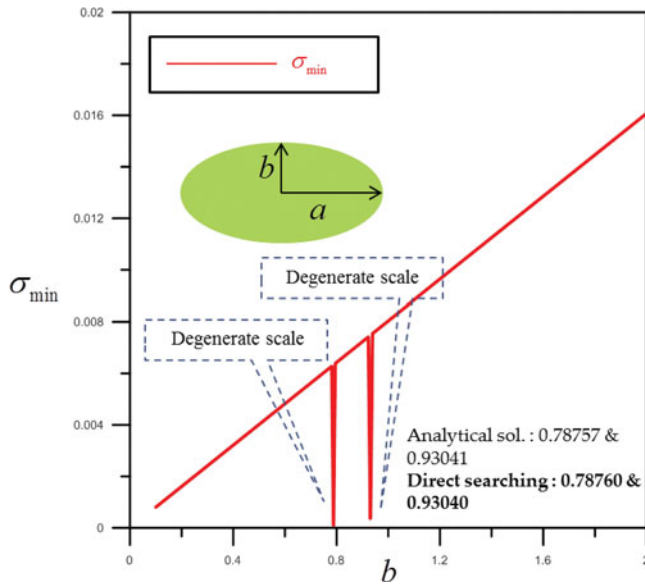


Figure 5. The minimum singular value vs. the length of semi-minor axis by using the direct searching technique.

below:

$$\mathbf{K}_{30^\circ} = \begin{bmatrix} \cos(-30^\circ) & \sin(-30^\circ) \\ -\sin(-30^\circ) & \cos(-30^\circ) \end{bmatrix}$$

$$\mathbf{K}_{0^\circ} = \begin{bmatrix} \cos(-30^\circ) & -\sin(-30^\circ) \\ \sin(-30^\circ) & \cos(-30^\circ) \end{bmatrix}, \quad (79)$$

$$\mathbf{K}_{60^\circ} = \begin{bmatrix} \cos(-60^\circ) & \sin(-60^\circ) \\ -\sin(-60^\circ) & \cos(-60^\circ) \end{bmatrix}$$

$$\mathbf{K}_{0^\circ} = \begin{bmatrix} \cos(-60^\circ) & -\sin(-60^\circ) \\ \sin(-60^\circ) & \cos(-60^\circ) \end{bmatrix}. \quad (80)$$

We also plot the Mohr's circle to demonstrate that \mathbf{K} matrix is the second-order tensor as shown in Figure 6.

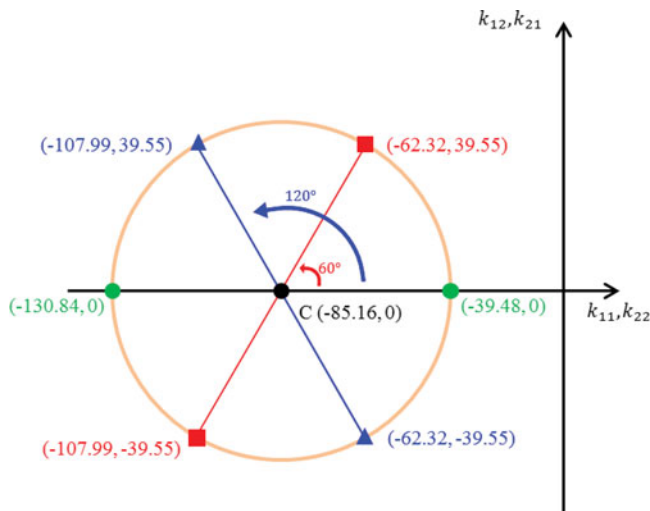


Figure 6. Mohr's circle representation for \mathbf{K} matrices with respect to three different observer systems.

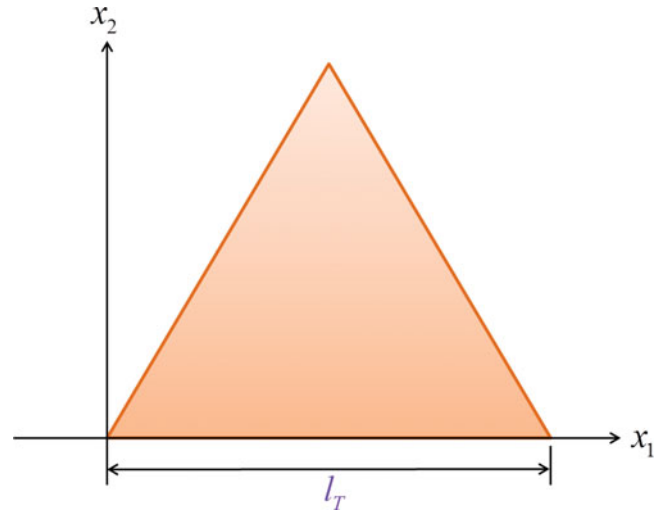


Figure 7. A plane elasticity problem of a triangular domain.

5.3. Degenerate scales of a triangle

Since the degenerate kernels of circular and elliptical cases are available, we can derive the analytical degenerate scale for these two cases. Therefore, the analytical result can be used for comparison with the numerical results when the numerical method is developed for solving arbitrary geometry. The two-trials technique and the direct searching technique can deal with problems with arbitrary boundary. In this example, we consider a triangle domain as shown in Figure 7 and the ordinary length of each boundary l_T is equal to 1.

The two-trials technique of the indirect BEM yields:

$$\mathbf{K} = \begin{bmatrix} 8.57868 & 0.0000 \\ 0.0000 & 8.57868 \end{bmatrix}, \quad (81)$$

and the expansion ratio is $d^* = 3.00004$. Therefore, the degenerate scale of a triangle domain is 3.00004. It is interesting to find that this case has double roots.

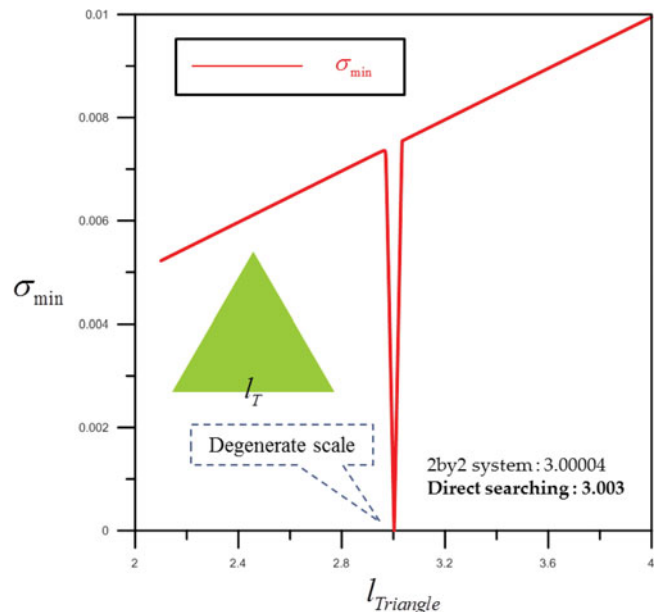


Figure 8. The minimum singular value vs. the length of side by using the direct searching technique.

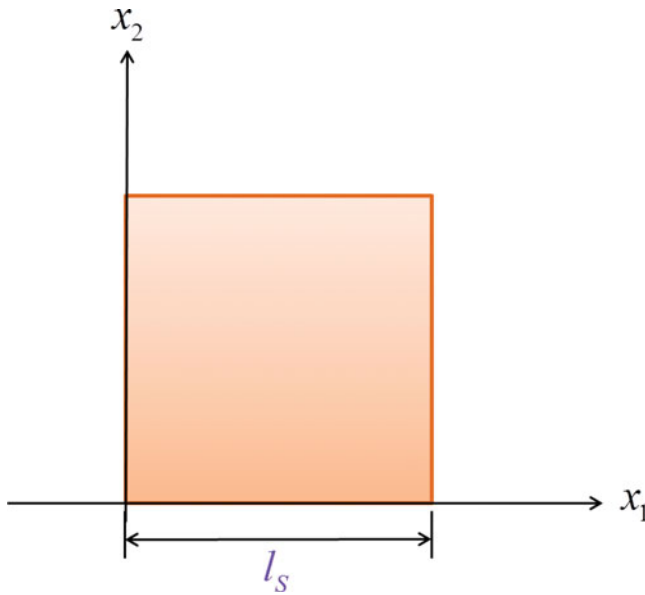


Figure 9. A plane elasticity problem of a square domain.

According to the direct searching technique, we find the degenerate scale of 3.003. The result is shown in Figure 8. It is clear to see that the results of the two techniques (direct searching and two-trials) match well.

5.4. Degenerate scales of a square

Here, we also consider a square domain as shown in Figure 9 and the ordinary length of each boundary l_s is equal to 1. By employing two trials of the indirect BEM, we have:

$$\mathbf{K} = \begin{bmatrix} 12.25125 & 0.00000 \\ 0.00000 & 12.25125 \end{bmatrix}, \quad (82)$$

and the expansion ratio is $d^* = 2.15823$. Therefore, the degenerate scale of a square domain is 2.15823, which is close to the

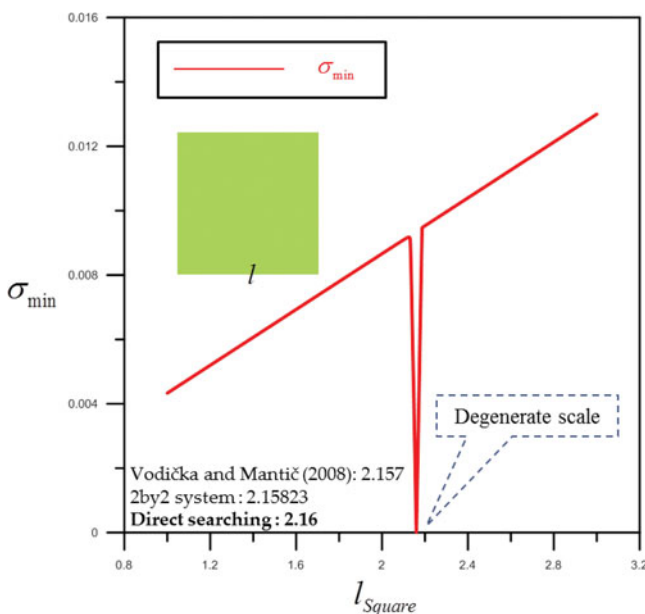


Figure 10. The minimum singular value vs. the length of side by using the direct searching technique.

numerical solution of 2.15694 [17]. We find that the square case also has double roots.

According to the direct searching technique, we find the degenerate scale of 2.16 as shown in Figure 10. Agreement is also made.

6. Conclusions

Not only was a degenerate kernel for the 2D Kelvin solution using the polar coordinates reviewed but also the new derivation for the degenerate kernel in terms of elliptical coordinates was completed. Degenerate scales for a circle and an ellipse in the indirect BIEM/BEM were analytically derived. Range deficiency for the single-layer integral representation was also examined. This article provided a deep understanding and proposed an alternative way to determine the degenerate scale in the indirect BIEM/BEM by using the degenerate kernel. By way of only two-trials of rigid body modes, we also can reduce the degenerate-scale problem to an eigenproblem of 2×2 matrix for a 2D elasticity problem. Following this idea, we can find the degenerate scales in the discrete system after we obtain the eigenvalue. Several different geometries: a circle, an ellipse, an equilateral triangle, and square were demonstrated to see the validity of our formulations.

Funding

Financial support from the Ministry of Science and Technology under Grant No. NSC 101-2221-E019-050 -MY3 for National Taiwan Ocean University is gratefully acknowledged.

References

- [1] T.C. Ting, Elastic wedge subjected to antiplane shear tractions—A paradox explained, *Q. J. Mech. Appl. Math.*, vol. 38, pp. 245–255, 1985.
- [2] M. Costabel and M. Dauge, Invertibility of the biharmonic single layer potential operator, *Integr. Equ. Oper. Theory*, vol. 24, pp. 46–67, 1996.
- [3] S. Christiansen, Integral equations without a unique solution can be made useful for solving some plane harmonic problems, *J. Inst. Math. Appl.*, vol. 16, pp. 59–143, 1975.
- [4] S. Christiansen, Detecting non-uniqueness of solutions to biharmonic integral equations through SVD, *J. Comput. Appl. Math.*, vol. 134, pp. 23–35, 2001.
- [5] W.J. He, A necessary and sufficient boundary integral formulation for plane elasticity problems, *Commun. Numer. Methods Eng.*, vol. 12, pp. 413–424, 1996.
- [6] W.J. He, H.J. Ding, and H.C. Hu, Non-equivalence of the conventional boundary integral formulation and its elimination for plane elasticity problems, *Comput. Struct.*, vol. 59, pp. 1059–1062, 1996.
- [7] M.A. Jaswon and G.T. Symm, *Integral Equation Methods in Potential Theory and Elastostatics*, Academic, London, 1977.
- [8] R. Vodička and V. Mantič, On invertibility of elastic single-layer potential operator, *J. Elast.*, vol. 74, pp. 147–173, 2004.
- [9] S. Christiansen, On two methods for elimination of non-unique solutions of an integral equation with logarithmic kernel, *Appl. Anal.*, vol. 13, pp. 1–18, 1982.
- [10] J.T. Chen, S.R. Kuo, and J.H. Lin, Analytical study and numerical experiments for degenerate scale problems in the boundary element method for two-dimensional elasticity, *Int. J. Numer. Methods Eng.*, vol. 54, pp. 1669–1681, 2002.

- [11] J.T. Chen, S.R. Lin, and K.H. Chen, Degenerate scale problem when solving Laplace's equation by BEM and its treatment, *Int. J. Numer. Methods Eng.*, vol. 62, pp. 233–261, 2005.
- [12] J.T. Chen, W.C. Shen, and A.C. Wu, Null-field integral equations for stress field around circular holes under anti-plane, *Eng. Anal. Boundary Elem.*, vol. 30, pp. 205–217, 2005.
- [13] W.J. He, H.J. Ding, and H.C. Hu, Degenerate scale and boundary element analysis of two dimensional potential and elasticity problems, *Comput. Struct.*, vol. 60, pp. 155–158, 1996.
- [14] S.R. Kuo, J.T. Chen, and S. K. Kuo, Linkage between the unit logarithmic capacity in the theory of complex variables and the degenerate scale in the BEM/BIEMs, *Appl. Math. Lett.*, vol. 26, pp. 929–938, 2013.
- [15] C. Constanda, On nonunique solutions of weakly singular integral equations in plane elasticity, *Quart. J. Mech. Math.*, vol. 47, pp. 261–268, 1994.
- [16] C. Constanda, Integral equations of the first kind in plane elasticity, *Q. Appl. Math.*, vol. 47, pp. 783–793, 1995.
- [17] R. Vodička and V. Mantič, On solvability of a boundary integral equation of the first kind for Dirichlet boundary value problems in plane elasticity, *Comput. Mech.*, vol. 41, pp. 817–826, 2008.
- [18] S.J. Zhou, S.X. Sun, and Z.Y. Cao, The boundary contour method base on the equivalent boundary integral equation for 2-D linear elasticity, *Commun. Numer. Methods Eng.*, vol. 15, pp. 811–821, 1999.
- [19] J.T. Chen, H. Han, S.R. Kuo, and S.K. Kao, Regularization methods for ill-conditioned system of the integral equation of the first kind with the logarithmic kernel, *Inverse Prob. Sci. Eng.*, vol. 22, pp. 1176–1195, 2014.
- [20] R. Vodička and M. Petrik, Degenerate scales for boundary value problems in anisotropic elasticity, *Int. J. Solids Struct.*, vol. 52, pp. 209–219, 2015.
- [21] Y.Z. Chen, Z.X. Wang, and X.Y. Lin, Numerical examination for degenerate scale problem for ellipse-shaped ring region in BIE, *Int. J. Numer. Methods Eng.*, vol. 71, pp. 1023–1230, 2007.
- [22] J.A. Cochran, *Applied Mathematics: Principles, Techniques, and Applications*, Wadsworth, Belmont, CA, 1982.
- [23] J.T. Chen, Y.T. Lee, and K.H. Chou, Revisit of two classical elasticity problems by using the null-field boundary integral equations, *J. Mech.*, vol. 26, pp. 393–401, 2010.
- [24] Z.C. Li, M.G. Lee, and J.T. Chen, New series expansions for fundamental solutions of linear elastostatics in 2D, *Computing*, vol. 92, pp. 199–224, 2010.
- [25] J.T. Chen, Y.T. Lee, and J.W. Lee, Torsional rigidity of an elliptic bar with multiple elliptic inclusions using a null-field integral approach, *Comput. Mech.*, vol. 46, pp. 511–519, 2010.
- [26] H.-K. Hong and J.T. Chen, Derivations of integral equations of elasticity, *J. Eng. Mech.*, vol. 114, pp. 1028–1044, 1988.

Appendix

Degenerate kernels for the 2D elasticity problem using the elliptic coordinates

$U_{11}(\mathbf{s}, \mathbf{x})$

$$\begin{aligned}
 & \left[-\frac{1}{8\pi G(1-\nu)} \left[(3-4\nu) \left(\bar{\xi} + \ln \frac{c}{2} - \sum_{m=1}^{\infty} \frac{2}{m} e^{-m\bar{\xi}} \cosh(m\xi) \cos(m\eta) \cos(m\bar{\eta}) - \sum_{m=1}^{\infty} \frac{2}{m} e^{-m\bar{\xi}} \sinh(m\xi) \sin(m\eta) \sin(m\bar{\eta}) \right) \right. \right. \\
 & - \frac{c^2}{4J^2} \left(-\sum_{m=1}^{\infty} e^{-m\bar{\xi}} \cosh((m+2)\xi) \cos((m-2)\eta) \cos(m\bar{\eta}) + \sum_{m=1}^{\infty} e^{-m\bar{\xi}} \cosh((m-2)\xi) \cos((m+2)\eta) \cos(m\bar{\eta}) \right. \\
 & - \sum_{m=1}^{\infty} e^{-m\bar{\xi}} \sinh((m+2)\xi) \sin((m-2)\eta) \sin(m\bar{\eta}) + \sum_{m=1}^{\infty} e^{-m\bar{\xi}} \sinh((m-2)\xi) \sin((m+2)\eta) \sin(m\bar{\eta}) \\
 & + \sum_{m=1}^{\infty} e^{-m\bar{\xi}} \cosh((m+2)\xi) \cos(m\eta) \cos((m+2)\bar{\eta}) + \sum_{m=1}^{\infty} e^{-(m+2)\bar{\xi}} \cosh((m+2)\xi) \cos(m\eta) \cos(m\bar{\eta}) \\
 & - \sum_{m=1}^{\infty} e^{-m\bar{\xi}} \cosh(m\xi) \cos((m+2)\eta) \cos((m+2)\bar{\eta}) - \sum_{m=1}^{\infty} e^{-(m+2)\bar{\xi}} \cosh(m\xi) \cos((m+2)\eta) \cos(m\bar{\eta}) \\
 & + \sum_{m=1}^{\infty} e^{-m\bar{\xi}} \sinh((m+2)\xi) \sin(m\eta) \sin((m+2)\bar{\eta}) + \sum_{m=1}^{\infty} e^{-(m+2)\bar{\xi}} \sinh((m+2)\xi) \sin(m\eta) \sin(m\bar{\eta}) \\
 & - \sum_{m=1}^{\infty} e^{-m\bar{\xi}} \sinh(m\xi) \sin((m+2)\eta) \sin((m+2)\bar{\eta}) - \sum_{m=1}^{\infty} e^{-(m+2)\bar{\xi}} \sinh(m\xi) \sin((m+2)\eta) \sin(m\bar{\eta}) \\
 & \left. \left. + \cosh(2\xi) \cos(2\bar{\eta}) + \cosh(2\xi) + e^{-2\bar{\xi}} \cosh(2\xi) - \cos(2\eta) \cos(2\bar{\eta}) - \cos(2\eta) - e^{-2\xi} \cos(2\eta) \right) \right], \quad \bar{\xi} \geq \xi, \\
 & = \left[-\frac{1}{8\pi G(1-\nu)} \left[(3-4\nu) \left(\xi + \ln \frac{c}{2} - \sum_{m=1}^{\infty} \frac{2}{m} e^{-m\xi} \cosh(m\bar{\xi}) \cos(m\eta) \cos(m\bar{\eta}) - \sum_{m=1}^{\infty} \frac{2}{m} e^{-m\xi} \sinh(m\bar{\xi}) \sin(m\eta) \sin(m\bar{\eta}) \right) \right. \right. \\
 & - \frac{c^2}{4J^2} \left(+\sum_{m=1}^{\infty} e^{-(m-2)\xi} \cos((m+2)\eta) \cosh(m\bar{\xi}) \cos(m\bar{\eta}) - \sum_{m=1}^{\infty} e^{-(m+2)\xi} \cos((m-2)\eta) \cosh(m\bar{\xi}) \cos(m\bar{\eta}) \right. \\
 & + \sum_{m=1}^{\infty} e^{-(m-2)\xi} \sin((m+2)\eta) \sinh(m\bar{\xi}) \sin(m\bar{\eta}) - \sum_{m=1}^{\infty} e^{-(m+2)\xi} \sin((m-2)\eta) \sinh(m\bar{\xi}) \sin(m\bar{\eta}) \\
 & - \sum_{m=1}^{\infty} e^{-m\xi} \cos((m+2)\eta) \cosh((m+2)\bar{\xi}) \cos(m\bar{\eta}) - \sum_{m=1}^{\infty} e^{-(m-2)\xi} \cos(m\eta) \cosh((m-2)\bar{\xi}) \cos(m\bar{\eta}) \\
 & + \sum_{m=1}^{\infty} e^{-(m+2)\xi} \cos(m\eta) \cosh(m+2\bar{\xi}) \cos(m\bar{\eta}) + \sum_{m=1}^{\infty} e^{-m\xi} \cos((m-2)\eta) \cosh(m-2\bar{\xi}) \cos(m\bar{\eta}) \\
 & - \sum_{m=1}^{\infty} e^{-m\xi} \sin((m+2)\eta) \sinh((m+2)\bar{\xi}) \sin(m\bar{\eta}) - \sum_{m=1}^{\infty} e^{-(m-2)\xi} \sin(m\eta) \sinh((m-2)\bar{\xi}) \sin(m\bar{\eta}) \\
 & + \sum_{m=1}^{\infty} e^{-(m+2)\xi} \sin(m\eta) \sinh((m+2)\bar{\xi}) \sin(m\bar{\eta}) + \sum_{m=1}^{\infty} e^{-m\xi} \sin((m-2)\eta) \sinh((m-2)\bar{\xi}) \sin(m\bar{\eta}) \\
 & \left. \left. + \sinh(2\xi) \cos(2\eta) - \cos(2\eta) \cosh(2\bar{\xi}) - \cos(2\eta) + \cosh(2\xi) + e^{-2\xi} \cosh(2\bar{\xi}) \right) \right], \quad \bar{\xi} < \xi,
 \end{aligned}$$

$U_{12}(\mathbf{s}, \mathbf{x})$

$$\begin{aligned}
& \left[\frac{1}{8\pi G(1-\nu)} \left[\frac{c^2}{4J^2} \left(\sum_{m=1}^{\infty} e^{-m\bar{\xi}} \sinh((m+2)\xi) \sin((m-2)\eta) \cos(m\bar{\eta}) - \sum_{m=1}^{\infty} e^{-m\bar{\xi}} \sinh((m-2)\xi) \sin((m+2)\eta) \cos(m\bar{\eta}) \right. \right. \right. \\
& - \sum_{m=1}^{\infty} e^{-m\bar{\xi}} \cosh((m+2)\xi) \cos((m-2)\eta) \sin(m\bar{\eta}) + \sum_{m=1}^{\infty} e^{-m\bar{\xi}} \cosh((m-2)\xi) \cos((m+2)\eta) \sin(m\bar{\eta}) \\
& + \sum_{m=1}^{\infty} e^{-m\bar{\xi}} \cosh((m+2)\xi) \cos(m\eta) \sin((m+2)\bar{\eta}) + \sum_{m=1}^{\infty} e^{-(m+2)\bar{\xi}} \cosh((m+2)\xi) \cos(m\eta) \sin(m\bar{\eta}) \\
& - \sum_{m=1}^{\infty} e^{-m\bar{\xi}} \cosh(m\xi) \cos((m+2)\eta) \sin((m+2)\bar{\eta}) - \sum_{m=1}^{\infty} e^{-(m+2)\bar{\xi}} \cosh(m\xi) \cos((m+2)\eta) \sin(m\bar{\eta}) \\
& - \sum_{m=1}^{\infty} e^{-m\bar{\xi}} \sinh((m+2)\xi) \sin(m\eta) \cos((m+2)\bar{\eta}) - \sum_{m=1}^{\infty} e^{-(m+2)\bar{\xi}} \sinh((m+2)\xi) \sin(m\eta) \cos(m\bar{\eta}) \\
& + \sum_{m=1}^{\infty} e^{-m\bar{\xi}} \sinh(m\xi) \sin((m+2)\eta) \cos((m+2)\bar{\eta}) + \sum_{m=1}^{\infty} e^{-(m+2)\bar{\xi}} \sinh(m\xi) \sin((m+2)\eta) \cos(m\bar{\eta}) \\
& \left. \left. \left. + \cosh(2\xi) \sin(2\bar{\eta}) - \cos(2\eta) \sin(2\bar{\eta}) \right) \right], \quad \bar{\xi} \geq \xi, \\
& = \left[\frac{1}{8\pi G(1-\nu)} \left[\frac{c^2}{4J^2} \left(\sum_{m=1}^{\infty} e^{-(m-2)\xi} \sin((m+2)\eta) \cosh(m\bar{\xi}) \cos(m\bar{\eta}) - \sum_{m=1}^{\infty} e^{-(m+2)\xi} \sin((m-2)\eta) \cosh(m\bar{\xi}) \cos(m\bar{\eta}) \right. \right. \right. \\
& - \sum_{m=1}^{\infty} e^{-(m-2)\xi} \cos((m+2)\eta) \sinh(m\bar{\xi}) \sin(m\bar{\eta}) + \sum_{m=1}^{\infty} e^{-(m+2)\xi} \cos((m-2)\eta) \sinh(m\bar{\xi}) \sin(m\bar{\eta}) \\
& + \sum_{m=0}^{\infty} e^{-m\xi} \cos((m+2)\eta) \sinh((m+2)\bar{\xi}) \sin(m\bar{\eta}) + \sum_{m=1}^{\infty} e^{-(m-2)\xi} \cos(m\eta) \sinh((m-2)\bar{\xi}) \sin(m\bar{\eta}) \\
& - \sum_{m=1}^{\infty} e^{-(m+2)\xi} \cos(m\eta) \sinh((m+2)\bar{\xi}) \sin(m\bar{\eta}) - \sum_{m=1}^{\infty} e^{-m\xi} \cos((m-2)\eta) \sinh((m-2)\bar{\xi}) \sin(m\bar{\eta}) \\
& - \sum_{m=1}^{\infty} e^{-m\xi} \sin((m+2)\eta) \cosh((m+2)\bar{\xi}) \cos(m\bar{\eta}) - \sum_{m=1}^{\infty} e^{-(m-2)\xi} \sin(m\eta) \cosh((m-2)\bar{\xi}) \cos(m\bar{\eta}) \\
& + \sum_{m=1}^{\infty} e^{-(m+2)\xi} \sin(m\eta) \cosh((m+2)\bar{\xi}) \cos(m\bar{\eta}) + \sum_{m=1}^{\infty} e^{-m\xi} \sin((m-2)\eta) \cosh((m-2)\bar{\xi}) \cos(m\bar{\eta}) \\
& \left. \left. \left. + \cosh(2\xi) \sin(2\eta) - \sin(2\eta) \cosh(2\bar{\xi}) \right) \right], \quad \bar{\xi} < \xi,
\end{aligned}$$

$U_{21}(\mathbf{s}, \mathbf{x})$

$$\begin{aligned}
& \left[\frac{1}{8\pi G(1-\nu)} \left[\frac{c^2}{4J^2} \left(\sum_{m=1}^{\infty} e^{-m\bar{\xi}} \sinh((m+2)\xi) \sin((m-2)\eta) \cos(m\bar{\eta}) - \sum_{m=1}^{\infty} e^{-m\bar{\xi}} \sinh((m-2)\xi) \sin((m+2)\eta) \cos(m\bar{\eta}) \right) \right. \right. \\
& - \sum_{m=1}^{\infty} e^{-m\bar{\xi}} \cosh((m+2)\xi) \cos((m-2)\eta) \sin(m\bar{\eta}) + \sum_{m=1}^{\infty} e^{-m\bar{\xi}} \cosh((m-2)\xi) \cos((m+2)\eta) \sin(m\bar{\eta}) \\
& + \sum_{m=1}^{\infty} e^{-m\bar{\xi}} \cosh((m+2)\xi) \cos(m\eta) \sin((m+2)\bar{\eta}) + \sum_{m=1}^{\infty} e^{-(m+2)\bar{\xi}} \cosh((m+2)\xi) \cos(m\eta) \sin(m\bar{\eta}) \\
& - \sum_{m=1}^{\infty} e^{-m\bar{\xi}} \cosh(m\xi) \cos((m+2)\eta) \sin((m+2)\bar{\eta}) - \sum_{m=1}^{\infty} e^{-(m+2)\bar{\xi}} \cosh(m\xi) \cos((m+2)\eta) \sin(m\bar{\eta}) \\
& - \sum_{m=1}^{\infty} e^{-m\bar{\xi}} \sinh((m+2)\xi) \sin(m\eta) \cos((m+2)\bar{\eta}) - \sum_{m=1}^{\infty} e^{-(m+2)\bar{\xi}} \sinh((m+2)\xi) \sin(m\eta) \cos(m\bar{\eta}) \\
& + \sum_{m=1}^{\infty} e^{-m\bar{\xi}} \sinh(m\xi) \sin((m+2)\eta) \cos((m+2)\bar{\eta}) + \sum_{m=1}^{\infty} e^{-(m+2)\bar{\xi}} \sinh(m\xi) \sin((m+2)\eta) \cos(m\bar{\eta}) \\
& \left. + \cosh(2\xi) \sin(2\bar{\eta}) - \cos(2\eta) \sin(2\bar{\eta}) \right], \quad \bar{\xi} \geq \xi, \\
& = \left[\frac{1}{8\pi G(1-\nu)} \left[\frac{c^2}{4J^2} \left(\sum_{m=1}^{\infty} e^{-(m-2)\xi} \sin((m+2)\eta) \cosh(m\bar{\xi}) \cos(m\bar{\eta}) - \sum_{m=1}^{\infty} e^{-(m+2)\xi} \sin((m-2)\eta) \cosh(m\bar{\xi}) \cos(m\bar{\eta}) \right) \right. \right. \\
& - \sum_{m=1}^{\infty} e^{-(m-2)\xi} \cos((m+2)\eta) \sinh(m\bar{\xi}) \sin(m\bar{\eta}) + \sum_{m=1}^{\infty} e^{-(m+2)\xi} \cos((m-2)\eta) \sinh(m\bar{\xi}) \sin(m\bar{\eta}) \\
& + \sum_{m=0}^{\infty} e^{-m\xi} \cos((m+2)\eta) \sinh((m+2)\bar{\xi}) \sin(m\bar{\eta}) + \sum_{m=1}^{\infty} e^{-(m-2)\xi} \cos(m\eta) \sinh((m-2)\bar{\xi}) \sin(m\bar{\eta}) \\
& - \sum_{m=1}^{\infty} e^{-(m+2)\xi} \cos(m\eta) \sinh((m+2)\bar{\xi}) \sin(m\bar{\eta}) - \sum_{m=1}^{\infty} e^{-m\xi} \cos((m-2)\eta) \sinh((m-2)\bar{\xi}) \sin(m\bar{\eta}) \\
& - \sum_{m=1}^{\infty} e^{-m\xi} \sin((m+2)\eta) \cosh((m+2)\bar{\xi}) \cos(m\bar{\eta}) - \sum_{m=1}^{\infty} e^{-(m-2)\xi} \sin(m\eta) \cosh((m-2)\bar{\xi}) \cos(m\bar{\eta}) \\
& + \sum_{m=1}^{\infty} e^{-(m+2)\xi} \sin(m\eta) \cosh((m+2)\bar{\xi}) \cos(m\bar{\eta}) + \sum_{m=1}^{\infty} e^{-m\xi} \sin((m-2)\eta) \cosh((m-2)\bar{\xi}) \cos(m\bar{\eta}) \\
& \left. + \cosh(2\xi) \sin(2\eta) - \sin(2\eta) \cosh(2\bar{\xi}) \right], \quad \bar{\xi} < \xi,
\end{aligned}$$

$U_{22}(\mathbf{s}, \mathbf{x})$

$$\begin{aligned}
& \left[-\frac{1}{8\pi G(1-\nu)} \left[(3-4\nu) \left(\bar{\xi} + \ln \frac{c}{2} - \sum_{m=1}^{\infty} \frac{2}{m} e^{-m\bar{\xi}} \cosh(m\xi) \cos(m\eta) \cos(m\bar{\eta}) - \sum_{m=1}^{\infty} \frac{2}{m} e^{-m\bar{\xi}} \sinh(m\xi) \sin(m\eta) \sin(m\bar{\eta}) \right) \right. \right. \\
& - \frac{c^2}{4J^2} \left(\sum_{m=1}^{\infty} e^{-m\bar{\xi}} \cosh((m+2)\xi) \cos((m-2)\eta) \cos(m\bar{\eta}) - \sum_{m=1}^{\infty} e^{-m\bar{\xi}} \cosh((m-2)\xi) \cos((m+2)\eta) \cos(m\bar{\eta}) \right. \\
& + \sum_{m=1}^{\infty} e^{-m\bar{\xi}} \sinh((m+2)\xi) \sin((m-2)\eta) \sin(m\bar{\eta}) - \sum_{m=1}^{\infty} e^{-m\bar{\xi}} \sinh((m-2)\xi) \sin((m+2)\eta) \sin(m\bar{\eta}) \\
& - \sum_{m=1}^{\infty} e^{-m\bar{\xi}} \sinh((m+2)\xi) \sin(m\eta) \sin((m+2)\bar{\eta}) - \sum_{m=1}^{\infty} e^{-(m+2)\bar{\xi}} \sinh((m+2)\xi) \sin(m\eta) \sin(m\bar{\eta}) \\
& + \sum_{m=1}^{\infty} e^{-m\bar{\xi}} \sinh(m\xi) \sin((m+2)\eta) \sin((m+2)\bar{\eta}) + \sum_{m=1}^{\infty} e^{-(m+2)\bar{\xi}} \sinh(m\xi) \sin((m+2)\eta) \sin(m\bar{\eta}) \\
& - \sum_{m=1}^{\infty} e^{-m\bar{\xi}} \cosh((m+2)\xi) \cos(m\eta) \cos((m+2)\bar{\eta}) - \sum_{m=1}^{\infty} e^{-(m+2)\bar{\xi}} \cosh((m+2)\xi) \cos(m\eta) \cos(m\bar{\eta}) \\
& \left. \left. + \sum_{m=1}^{\infty} e^{-m\bar{\xi}} \cosh(m\xi) \cos((m+2)\eta) \cos((m+2)\bar{\eta}) + \sum_{m=1}^{\infty} e^{-(m+2)\bar{\xi}} \cosh(m\xi) \cos((m+2)\eta) \cos(m\bar{\eta}) \right] \right. \\
& \left. + \cosh(2\xi) - \cosh(2\xi) \cos(2\bar{\eta}) - e^{-2\bar{\xi}} \cosh(2\xi) - \cos(2\eta) + \cos(2\eta) \cos(2\bar{\eta}) + e^{-2\bar{\xi}} \cos(2\eta) \right], \quad \bar{\xi} \geq \xi, \\
& - \frac{1}{8\pi G(1-\nu)} \left[(3-4\nu) \left(\xi + \ln \frac{c}{2} - \sum_{m=1}^{\infty} \frac{2}{m} e^{-m\xi} \cosh(m\bar{\xi}) \cos(m\eta) \cos(m\bar{\eta}) - \sum_{m=1}^{\infty} \frac{2}{m} e^{-m\xi} \sinh(m\bar{\xi}) \sin(m\eta) \sin(m\bar{\eta}) \right) \right. \\
& - \frac{c^2}{4J^2} \left(-\sum_{m=1}^{\infty} e^{-(m-2)\xi} \cos((m+2)\eta) \cosh(m\bar{\xi}) \cos(m\bar{\eta}) + \sum_{m=1}^{\infty} e^{-(m+2)\xi} \cos((m-2)\eta) \cosh(m\bar{\xi}) \cos(m\bar{\eta}) \right. \\
& - \sum_{m=1}^{\infty} e^{-(m-2)\xi} \sin((m+2)\eta) \sinh(m\bar{\xi}) \sin(m\bar{\eta}) + \sum_{m=1}^{\infty} e^{-(m+2)\xi} \sin((m-2)\eta) \sinh(m\bar{\xi}) \sin(m\bar{\eta}) \\
& + \sum_{m=1}^{\infty} e^{-m\xi} \sin((m+2)\eta) \sinh((m+2)\bar{\xi}) \sin(m\bar{\eta}) + \sum_{m=1}^{\infty} e^{-(m-2)\xi} \sin(m\eta) \sinh((m-2)\bar{\xi}) \sin(m\bar{\eta}) \\
& - \sum_{m=1}^{\infty} e^{-(m+2)\xi} \sin(m\eta) \sinh((m+2)\bar{\xi}) \sin(m\bar{\eta}) - \sum_{m=1}^{\infty} e^{-m\xi} \sin((m-2)\eta) \sinh((m-2)\bar{\xi}) \sin(m\bar{\eta}) \\
& + \sum_{m=1}^{\infty} e^{-m\xi} \cos((m+2)\eta) \cosh((m+2)\bar{\xi}) \cos(m\bar{\eta}) + \sum_{m=1}^{\infty} e^{-(m-2)\xi} \cos((m)\eta) \cosh((m-2)\bar{\xi}) \cos(m\bar{\eta}) \\
& - \sum_{m=1}^{\infty} e^{-(m+2)\xi} \cos(m\eta) \cosh((m+2)\bar{\xi}) \cos(m\bar{\eta}) - \sum_{m=1}^{\infty} e^{-m\xi} \cos((m-2)\eta) \cosh((m-2)\bar{\xi}) \cos(m\bar{\eta}) \\
& \left. \left. - \sinh(2\xi) \cos(2\eta) + \cos(2\eta) \cosh(2\bar{\xi}) - \cos(2\eta) + \cosh(2\xi) - e^{-2\xi} \cosh(2\bar{\xi}) \right] \right], \quad \bar{\xi} < \xi,
\end{aligned}$$

where $U_{ij}(\mathbf{x}, \mathbf{s}) = -\frac{1}{8\pi G(1-\nu)} \left(\kappa \delta_{ij} \ln r - \frac{y_i y_j}{r^2} \right)$.